16th World Conference on Earthquake, 16WCEE 2017

Santiago Chile, January 9th to 13th 2017

Paper N° 2774 (Abstract ID)

Registration Code: S-XXXXXXXX

FORCE-DISPLACEMENT DECOUPLED CONTROL OF ENGINEERING STRUCTURES WITH MULTI-DEGREE-OF-FREEDOM TESTING

H. Zhou*(1), M. Li(2), T. Wang(3)

(1) *Assistant researcher, Key Laboratory of Earthquake Engineering and Engineering Vibration, Institute of Engineering Mechanics, CEA, Sanhe 065201, zhouhuimeng@iem.ac.cn*

(2) *Master student, Key Laboratory of Earthquake Engineering and Engineering Vibration, Institute of Engineering Mechanics, CEA, Sanhe 065201, dqsymengyou@vip.qq.com*

(3) *Researcher, Key Laboratory of Earthquake Engineering and Engineering Vibration, Institute of Engineering Mechanics, CEA, Sanhe 065201,wangtao@iem.ac.cn*

Abstract

Engineering structures sustains the spatial forces from the gravity, wind, earthquakes and so on. To examine the performance of such structural members, the forces in all six degrees of freedom(DOF) need to be exerted synchronously on the tested member. Because of the rigidity of the specimen, there are strong coupling effects among the six DOFs, which brings significant difficulty in the control of traditional linear actuators. To sovle this problem, the force-displacement double closed-loop hybrid control strategy is proposed in this study, by considering both mateiral and geometric nonlinearities. The proposed force-displacement decoupled control method is validated using a small scale specimen test, and the feasibility of this decoupling control method is proved by the test results.

Keywords: Cyclic test, Multi-degree-of-freedom, Decoupling control, Displacement-force decoupled control

1. Introduction

Previous severe earthquakes have caused massive failure of engineering structures. It is urgent and necessary to carry out the experimental study to examine the seismic performance of these structures. To do this, the spatial load conditions on specimens shall be reproduced by loading devices. Earthquake simulation shaking tables can be applied for the multi-DOF vibration input[1]. But the size and weight of the model is limited. Quasi-static test devices and similar facilities for pseudo-dynamic testing, although having large loading capacity, are difficult to be re-assembled for the multi-DOF loading because of actuator-specimen coupling effect and the strong interaction among linear actuators themselves[2-7].

Concrete specimens are often featured with large stiffness which is difficult to control for most hydraulic actuators due to their limited oil-column stiffness. The force control might be an option. For example, a concrete pier could be loaded in the axial direction by use of a force-controlled actuator, while tested in the shear direction by a displacement-controlled actuator, so called displacement-force mixed control[8-9]. However, when more degrees of freedom are included at one single loading point, the actuators will be coupled. For example, if the bending, axial load and shear load are simultaneously controlled by three actuators. The two actuators used to control the bending will be used to control either the axial load or the shear load. Under such coupled condition, it’s difficult to realize the force-control in one direction while a displacement-control in the other.

To solve such challenge, some special facilities and control methods were developed recently. Nakata et al.[8] proposed a force-displacement mixed control method applied in the Load and Boundary Condition Box (LBCB) device, in which the force and displacement control was achieved in each Cartesian coordinate axis of a loading point. The loading scheme adopts the displacement priority. Once the target displacements are realized, an iterative procedure is taken to achieve the force target subsequently. By using this method, the force and displacement control of all 6 DOFs can be realized simultaneously. Note that the conversion between the actuator space feedbacks and the Cartesian coordinate targets is achieved iteratively by updating the transfer matrix[10].

Tan et al.[11] proposed a double closed-loop control strategy to realize the force-displacement hybrid control, in which the inner loop is the force control and the outer loop is the displacement control. Zeng et al.[12] applied this strategy in the horizontal and vertical DOF pseudo-dynamic tests and the quasi-static tests. Pan et al.[3] proposed a force-displacement mixed control method, which uses the displacement control in the main degree of freedom, and uses the force control in other degrees of freedom. Through iteration, it was ensured that the forces are loaded proportionally.

In order to avoid repeated loading caused by the iteration, a multi-DOF displacement-force hybrid control is proposed in this paper. This method uses the initial stiffness matrix to approximate the force-displacement relationship, and use the linearized coordinate transform matrix to approximate the geometric nonlinearities between the global coordinate system and the actuator expansion increment. These simplifications will decrease the control effect in open-loop system. In order to get good decoupling control effect, the outer closed-loop controller is used to correct the error caused by material and geometric nonlinearities. This method replaces the iteration to solve the nonlinear function for Multi-DOF loading system. The robustness controller is used to guarantee the uniform convergence of the control process. It has better performance than the repetitive loading in the iteration, because the repetitive loading will cause the inaccuracy for the path-dependent specimen. The conversion between the actuator space and the Cartesian system is developed considering a Stewart-based loading facility. The proposed system is finally demonstrated by a small-scale specimen loaded in all six-DOFs.

2. Force-Displacement Decoupled Control Method

The scheme of multi-DOF force-displacement hybrid control is shown in Figure 1. 6-DOF force-displacement hybrid control is discussed as an example. The 6-DOF loading system includes six actuators which are deployed as the Stewart mechanism. They are controlled in a displacement manner, while the outer-loop is a either a force or a displacement controller. The PI control method is used to design the outer-loop robust controller. The force and displacement feedback signals $\mathbf{Y}^{\mathrm{R}}_{i+1}$ are compared to the command $\mathbf{Y}_{i+1}$. The error $\mathbf{e}_{\mathrm{i+1}}$ between them are sent through the robust controller to generate the command signal. The commands first pass through the force-displacement conversion matrix designed by the initial stiffness matrix of the specimen to find each control mode, i.e., in displacement or in force. Before sent to the actuators, the command signal in the desired control mode is converted from the overall Cartesian coordinate to the actuator space by the conversion coefficient matrix $\mathbf{C}_{\mathrm{v}}^{\mathrm{T}}$, thus obtaining the command signal $\mathbf{I}^{\mathrm{c}}_{i+1}(t)$ for the six actuators. The actuator space response $\mathbf{I}^{\mathrm{R}}_{i+1}(t)$ is then measured by high-precision displacement/force sensors, which is transformed into the Cartesian coordinate, denoted as $\mathbf{Y}^{\mathrm{R}}_{i+1}$, and fed back to the robust controller.

First, the overall coordinate system is defined in the Cartesian coordinate system, and the axial extension of each actuator is defined as the actuator space. From the perspective of mechanical kinematics, the loading system with six DOF is a Stewart mechanism. The connecting point between the loading system and the specimen is defined as the control points. Now the problem is to solve the input position and orientation $\mathbf{q}^{\mathrm{R}}_{i+1}$ known the output position and orientation of the terminal $\mathbf{l}^{\mathrm{m}}_{i+1}(t)$. The geometrically nonlinear equation is usually solved by the iteration method. In this paper, the displacement response $\mathbf{l}^{\mathrm{m}}_{i+1}(t)$ of the actuators are measured, and the kinematic solution is directly realized by multiplying the conversion coefficient matrix $\mathbf{C}_{\mathrm{v}}$, thus the Cartesian coordinate displacement response $\mathbf{q}^{\mathrm{R}}_{i+1}(t)$ is obtained.

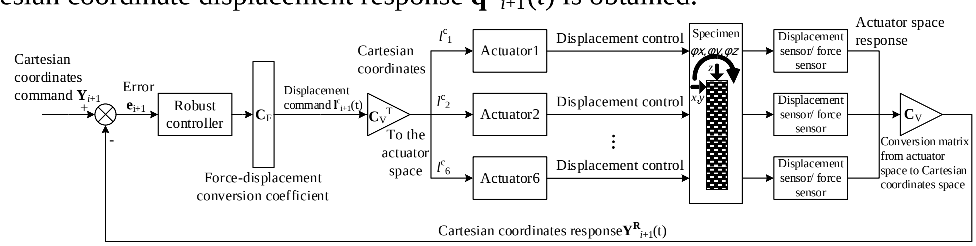

Fig. 1 – Robust control diagram of multiple DOF force-displacement hybrid control

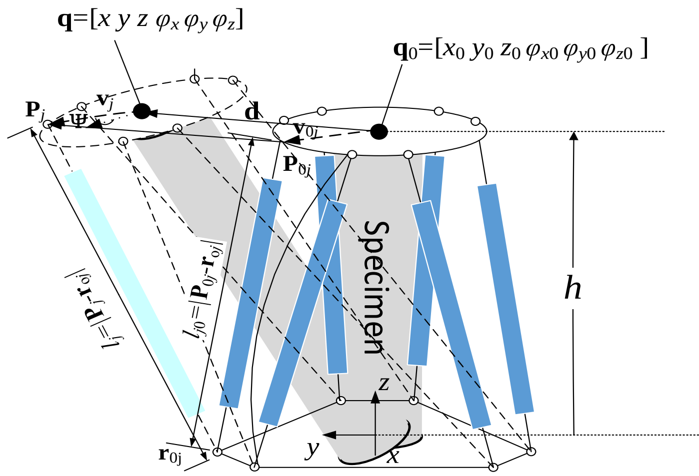

Fig. 2 – Coordinate conversion of the 6DOFs testing system

Take the system shown in Fig.2 as an example. x, y, …, φ_z are the target displacement of the 6-DOF system, corresponding to the horizontal x and y displacement, vertical z displacement and the rotational displacement of x, y, and z, which is the Cartesian coordinate displacement. l_1, l_2, …, l_6 are the original lengths of the actuators, while l'_1, l'_2, …, l'_6 are the current lengths of the actuators after loading. Δl_1, Δl_2, …, Δl_6 are the extension increments of the actuators relative to their initial positions. h is the height from the loading point to the ground. From Figure 2, it can be obtained that the translational DOFs $\mathbf{d}=[x\ y\ z]^{\mathrm{T}}$ in $\mathbf{q}$ can be written in terms of the initial and current control points as follows:

$$\mathbf{u} = \mathbf{u}_0 + \mathbf{d} \tag{1}$$

where $\mathbf{u}$ is the current control points, $\mathbf{u}_0$ is the initial control points. The vector $\mathbf{v}_{0j}$ from the initial control point $\mathbf{u}_0$ to the initial platform pin location $\mathbf{p}_{0j}$ of the j-th actuator can be obtained as

$$\mathbf{v}_{0j} = \mathbf{p}_{0j} - \mathbf{u}_0 \tag{2}$$

where $\mathbf{p}_{0j}$ is the initial platform pin location for the j-th actuator.

The rotational displacement (φ_x, φ_y, φ_z) results in a pure rotation of $\mathbf{v}_{0j}$.

$$\mathbf{v}_j = \boldsymbol{\psi}\mathbf{v}_{0j} \tag{3}$$

Where the rotational matrix Ψ follows the Roll-Pitch-Yaw rotational convention and is given by:

$$\boldsymbol{\psi} = \begin{bmatrix} \cos\varphi_z & -\sin\varphi_z & 0 \\ \sin\varphi_z & \cos\varphi_z & 0 \\ 0 & 0 & 1 \end{bmatrix} \begin{bmatrix} \cos\varphi_y & 0 & \sin\varphi_y \\ 0 & \cos\varphi_y & 0 \\ -\sin\varphi_y & 0 & 1 \end{bmatrix} \begin{bmatrix} 1 & 0 & 0 \\ 0 & \cos\varphi_x & -\sin\varphi_x \\ 0 & \sin\varphi_x & \cos\varphi_x \end{bmatrix} \tag{4}$$

The current platform pin location $\mathbf{P}_j$ for the j-th actuator due to the motion $\mathbf{q}$ is a sum of the translational displacement vector $\mathbf{u}$ at the control point and the rotated vector $\mathbf{v}_j$.

$$\mathbf{P}_j = \mathbf{u} + \mathbf{v}_j = \mathbf{u}_0 + \mathbf{d} + \boldsymbol{\psi}\mathbf{v}_{0j} \tag{5}$$

Finally, the current actuator length for the j-th actuator l_j can be written as follows:

$$l_j = \left|\mathbf{p}_j - \mathbf{r}_{0j}\right| = \left|\mathbf{d} - (\mathbf{I} - \boldsymbol{\psi})\mathbf{v}_{0j} + \mathbf{p}_{0j} - \mathbf{r}_{0j}\right| \tag{6}$$

where $\mathbf{r}_{0j}$ is the base pin location for the j-th actuator. The extension increment of the j-th actuator Δl_j can be written as

$$\Delta l_j = l_j - l_{0j} \tag{7}$$

Eq. (7) is a kinematic relationship between the j-th actuator length l_j and the global Cartesian coordinate vector $\mathbf{q}=[x, y, z, \varphi_x, \varphi_y, \varphi_z]^{\mathrm{T}}$.

In order to obtain the linear relationship of the coordinate transformation, the partial derivatives of Δl_1, Δl_2, …, Δl_6 with respect to x, y, …, φ_z are obtained. Assuming that the equilibrium position ($x=x_0$, $y=y_0$, $z=z_0$, …, $\varphi_z=\varphi_{z0}$) is the origin position, a constant conversion coefficient can be obtained using the conversion coefficient at the origin position. The coordinate transformation matrix can be obtained as:

$$\mathbf{C}_{\mathrm{v}}^{\mathrm{T}} = \begin{bmatrix} \frac{\partial \Delta l_1}{\partial x} & \frac{\partial \Delta l_1}{\partial y} & \cdots & \frac{\partial \Delta l_1}{\partial \varphi_z} \\ \frac{\partial \Delta l_2}{\partial x} & \frac{\partial \Delta l_2}{\partial y} & \cdots & \frac{\partial \Delta l_2}{\partial \varphi_z} \\ \vdots & \vdots & \vdots & \vdots \\ \frac{\partial \Delta l_6}{\partial x} & \frac{\partial \Delta l_6}{\partial y} & \cdots & \frac{\partial \Delta l_6}{\partial \varphi_z} \end{bmatrix} \tag{8}$$

The initial stiffness matrix of a specimen can be obtained by the perturbation method before the experiment, denoted as

$$\mathbf{K}_{\mathrm{E}} = \begin{bmatrix} k_{11} & k_{12} & \cdots & k_{16} \\ k_{21} & k_{22} & \cdots & k_{26} \\ \vdots & \vdots & \vdots & \vdots \\ k_{61} & k_{62} & \cdots & k_{66} \end{bmatrix} \tag{9}$$

Considering a real application where the horizontal *x* and *y* is in the displacement control mode, while the rest is in the force control. The force-displacement conversion coefficient matrix can be designed as

$$\mathbf{C}_{\mathrm{F}} = \frac{\mathbf{d}(s)}{\mathbf{F}(s)} = \begin{bmatrix} \mathbf{I}_{2\times2} & \mathbf{O}_{2\times4} \\ \mathbf{O}_{4\times2} & \bar{\mathbf{K}}_{4\times4}^{-1} \end{bmatrix} \tag{10}$$

where $\bar{\mathbf{K}}_{4\times4}$ is the part of the initial stiffness matrix $\mathbf{K}_{\mathrm{E}}$.

$$\bar{\mathbf{K}}_{4\times4} = \begin{bmatrix} k_{33} & k_{34} & k_{35} & k_{36} \\ k_{43} & k_{44} & k_{45} & k_{46} \\ k_{53} & k_{54} & k_{55} & k_{56} \\ k_{63} & k_{64} & k_{65} & k_{66} \end{bmatrix} \tag{11}$$

From Eq. (10), it can be seen that the horizontal DOFs are relatively independent in this force-displacement hybrid control strategy, and the transformation matrix from the Cartesian coordinate system to the actuator space is

$$\mathbf{l} = \mathrm{C}_{\mathrm{v}}^{\mathrm{T}} \cdot \mathbf{q} \tag{12}$$

In order to diminish the steady-state control error in the end of the loading step, the Proportional-Integral (PI) control scheme is applied:

$$\mathbf{G}_{\mathrm{c}}(s) = \frac{\begin{bmatrix} k_{\mathrm{P1}}s + k_{\mathrm{I1}} & 0 & \cdots & 0 \\ 0 & k_{\mathrm{P2}}s + k_{\mathrm{I2}} & \cdots & 0 \\ \vdots & \vdots & \cdots & \vdots \\ 0 & 0 & \cdots & k_{\mathrm{P6}}s + k_{\mathrm{I6}} \end{bmatrix}}{s} \tag{13}$$

3. Experimental Verification

3.1 Test equipment

The verification test was carried on a six-DOF platform system provided by Sanqiangtongwei electromechanical hydraulic technology company. A U-shaped reinforcing steel bar was used as the specimen. The loading equipment and the specimen are shown in Figure 3.

Figure. 3 – Loading equipment and specimen

The six-DOF motion platform system consists of the rigid motion platform, 6 servo motor actuators, the power amplifier, PLC controller, the communication equipment, the host computer and other components. It can achieve the decoupled displacement control in six-DOF, but cannot realize the force-displacement hybrid control. In the test system, the PLC controller is used as the internal closed-loop displacement controller and making the coordinate conversion. The other computer works as the outer-loop control program and its interface is established by C++ programming language. The program interface and the block diagram are shown in Figure 4 and Figure 5, respectively.

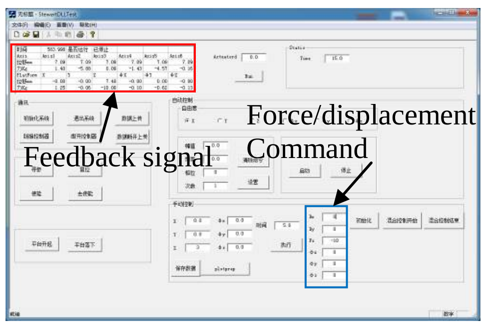

Figure. 4 – Control program interface

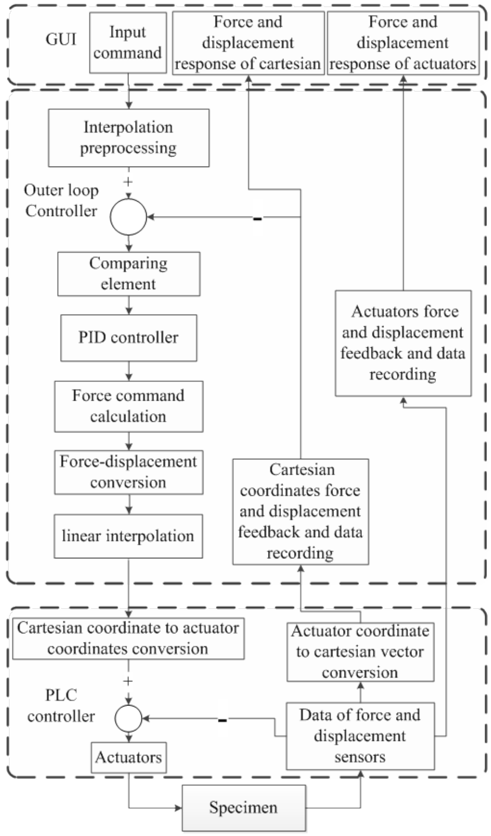

Figure. 5 – Control program interface and its block diagram

3.2 U-shaped reinforcing steel bar specimen test

A HPB300 reinforcing steel rebar is taken as the specimen. The diameter is 12mm, and its height is 500mm. The rebar was bended to a U-shape to decrease the axial stiffness. The stiffness matrix of the specimen is obtained by the perturbation method in the linear range of the specimen. The stiffness of every degree of freedom is obtained from the gradient of the linear fitted curve to the force-displacement curve:

$$\mathbf{K}_{\mathrm{E}} = \begin{bmatrix} -0.50 & -0.03 & 0.37 & 37.7 & 177.3 & -3.9 \\ 0 & -0.46 & -0.03 & -390 & -9.5 & -28.5 \\ 0.28 & -0.01 & -2.91 & -46.9 & 82.8 & 2.2 \\ -0.09 & -2.42 & 0.42 & -1766 & -73 & -15.2 \\ 2.96 & -0.15 & 0.56 & -134 & -1502 & 32.7 \\ -0.11 & -0.42 & 0.13 & -336 & 45 & -337 \end{bmatrix} \tag{14}$$

During the force-displacement hybrid loading, the control mode of the outer-loop in horizontal x and y direction is displacement control, and the rest are loaded in the force control mode. So the lower right corner partitioned matrix of the stiffness matrix $\mathbf{K}_{\mathrm{E}}$ is inversed to convert the force to the displacement command.

$$\overline{\mathbf{K}}_{4\times4}^{-1} = \begin{bmatrix} -0.346 & 0.013\times10^{-3} & -0.02\times10^{-3} & -0.0098\times10^{-3} \\ -0.07 & -0.62\times10^{-3} & 0.035\times10^{-3} & 0.279\times10^{-3} \\ -0.123 & 0.074\times10^{-3} & -0.679\times10^{-3} & -0.0996\times10^{-3} \\ -0.075 & 0.632\times10^{-3} & -0.133\times10^{-3} & -3.263\times10^{-3} \end{bmatrix} \tag{15}$$

The PI controller is used, whose parameters are

$$\mathbf{G}_{\mathrm{c}}(s) = \frac{0.5s+0.75}{s}\mathbf{I}_{6\times6} \tag{16}$$

In order to simply the control, the force-displacement conversion matrix only use the diagonal element

$$\mathbf{C}_{\mathrm{F}}=\begin{bmatrix}1 & 0 & 0 & 0 & 0 & 0\\ 0 & 1 & 0 & 0 & 0 & 0\\ 0 & 0 & -0.346 & 0 & 0 & 0\\ 0 & 0 & 0 & -0.62\times10^{-3} & 0 & 0\\ 0 & 0 & 0 & 0 & -0.679\times10^{-3} & 0\\ 0 & 0 & 0 & 0 & 0 & -3.263\times10^{-3}\end{bmatrix} \tag{17}$$

After the quasi-statically cyclic experiment, the force/displacement command are compared with response and shown in Figure 6. From Figure 6, it can be seen that both displacement and force responses track the command singals at the steady-state condition. The synchronously loading in the axial compression, shear, bend and torsion can be realized. It should be noted that the displacement command has been linearly interpolated in 5s when it is send to the PLC, which is the key to smooth the response of the actuators.

4. Conclusion

Aiming at solving the coupled problem during the synchronously loading for the piers or columns in axial, shear and bending DOFs, the force-displacement hybrid double closed-loop control strategy is proposed. The material and geometric nonlinearity of the loading device are considered in this decoupling control. A PI controller is used to reduce the error of multi-DOF synchronously loading. A small U-shaped reinforcing steel rebar specimen is loaded in six-DOF synchronously. The experimental results verified the feasibility and accuracy of this new method.

6. Acknowledgements

The research is financially supported by the Scientific Research Fund of Institute of Engineering Mechanics, China Earthquake Administration (Grant No. 2016B09, 2016A06) and National Science Foundation of China (51408565, 51378478, 51161120360).

7. References

[1] Lu X, Zou Y, Lu W, et al. (2007): Shaking table model test on Shanghai World Financial Center Tower. *Earthquake Engineering and Structural Dynamics*, *36*(4), 439-457.

[2] Qiu F, Li W, Pan P, Qian J(2002): Experimental tests on reinforced concrete columns under biaxial quasi-static loading. *Engineering Structures*, **24**(4), 419-428.

[3] Pan P, Zhao G, Lu X, Deng K(2014): Force-displacement mixed control for collapse tests of multistory buildings using quasi-static loading systems. *Earthquake Engineering and Structural Dynamics*, **43**(2), 287-300.

[4] Chen Z, Xu G, Wu B, et al. (2014): Equivalent force control method for substructure pseudo-dynamic test of a full-scale masonry structure. *Earthquake Engineering and Structural Dynamics*, **43**(7), 969-983.

[5] Chen J, Lin T, Chen P, Lin K, et al. (2009): Advanced seismic testing using the multi-axial testing system (MAST) in NCREE. *Proceedings of The 3rd International Conference on Advances in Experimental Structural Engineering*, San Francisco, USA.

[6] Mahin S, Nigbor R, Pancake C, et al. (2001). The development of the network for earthquake engineering simulation (NEES). *NEESgrid. org*.

[7] Nakata N, Spencer BF, Elnashai AS(2006): Mixed load/displacement control strategy for hybrid simulation. *4th International Conference on Earthquake Engineering*, Taipei, Taiwan, October 12-13, Paper No. 094.

[8] Pan P, Nakashima M, Tomofuji H(2005): Online test using displacement-force mixed control. *Earthquake Engineering Structural Dynamics*, **34**,869-888.

[9] Elwood KJ, Moehle JP(2008): Dynamic collapse analysis for a reinforced concrete frame sustaining shear and axial failures. *Earthquake Engineering and Structural Dynamics*, **37**,991-1012.

[10] Mahmoud HN, Elnashai AS, Spencer BF, et al. (2013): Hybrid simulation for earthquake response of semi-rigid partial-strength steel frames. *Journal of Structural Engineering*, **139**(7), 1134-1148.

[11] Tan X(2012): Pseudo-dynamic testing with control technique combining displacement outer loop and force inner loop. *Journal of Vibration and Shock*, **31**(14),16-21.(in Chinese)

[12] Zeng C, Wu B, Xu G, et al. (2014): Multi-axil dynamic structural testing system and its control strategies. *Journal of Vibration and Shock*, **33**(2),1-6.(in Chinese)